Biophysical Journal Volume 93 November 2007 3555–3566

An Unusual Transduction Pathway in Human Tonic Smooth Muscle Myosin

Miriam F. Halstead,* Katalin Ajtai,* Alan R. Penheiter,† Joshua D. Spencer,† Ye Zheng,* Emma A. Morrison,* and Thomas P. Burghardt*‡

*Biochemistry and Molecular Biology, †Anesthesiology, and ‡Physiology and Biomedical Engineering, Mayo Clinic College of Medicine, Rochester, Minnesota

ABSTRACT The motor protein myosin binds actin and ATP, producing work by causing relative translation of the proteins while transducing ATP free energy. Smooth muscle myosin has one of four heavy chains encoded by the MYH11 gene that differ at the C-terminus and in the active site for ATPase due to alternate splicing. A seven-amino-acid active site insert in phasic muscle myosin is absent from the tonic isoform. Fluorescence increase in the nucleotide sensitive tryptophan (NST) accompanies nucleotide binding and hydrolysis in several myosin isoforms implying it results from a common origin within the motor. A wild-type tonic myosin (smA) construct of the enzymatic head domain (subfragment 1 or S1) has seven tryptophan residues and nucleotide-induced fluorescence enhancement like other myosins. Three smA mutants probe the molecular basis for the fluorescence enhancement. W506+ contains one tryptophan at position 506 homologous to the NST in other myosins. W506F has the native tryptophans except phenylalanine replaces W506, and W506+(Y499F) is W506+ with phenylalanine replacing Y499. W506+ lacks nucleotide-induced fluorescence enhancement probably eliminating W506 as the NST. W506F has impaired ATPase activity but retains nucleotide-induced fluorescence enhancement. Y499F replacement in W506+ partially rescues nucleotide sensitivity demonstrating the role of Y499 as an NST facilitator. The exceptional response of W506 to active site conformation opens the possibility that phasic and tonic isoforms differ in how influences from active site ATPase propagate through the protein network.

INTRODUCTION

Myosin is a molecular motor binding ATP and actin to produce work using ATP free energy transduction at the active site to cause relative translation of the two proteins.

The multisubunit myosin is formed from a heavy chain (MHC) and two smaller light chains called essential (ELC) and regulatory (RLC). The MHC N-terminal globular head contains the ATPase site, the actin binding site, and lever arm where light chains bind. The lever arm swings during force production to propel bound actin. The MHC C-terminus forms a tail extending from the lever arm. The tail regulates and participates in myosin self-assembly first into dimers and then a thick filament. The thick filament backbone is made from associated myosin dimer tail domains with heads projecting outward to permit interaction of the actin binding site with adjacent actin (thin) filaments.

When phosphorylated, the RLC in smooth muscle triggers actin-activated myosin ATPase activity and myosin-based actin motility (1,2). Smooth muscle myosin contains one of four smooth muscle MHCs encoded by the MYH11 gene (3). The heavy-chain isoforms differ at the end of the tail near the C-terminus and in the active site. The active site difference consists of the seven amino acids QGPSFSY inserted or omitted between Thr-211 and Gly-212 and has been shown to correlate with tissue localization (4), enzyme kinetics (5–7), but not the step length of the motor (6). MHCs lacking (smA) or containing (smB) the insert are normally associated with tonic or phasic smooth muscles, respectively. ELC is expressed in two isoforms in vivo (LC_{17a} and LC_{17b}) but had no observed effect on in vitro myosin functionality (8). ELCs exchanged into permeabilized smooth muscle gave evidence for an isoform-specific effect on myosin functionality (9) but other evidences, reviewed by Arner et al. (10), have shown no correlation. Our work here investigating the nucleotide sensitive tryptophan (NST) residue in myosin will utilize a C-terminus truncated (short) human aorta smooth muscle MHC eliminating both the C-terminus differences in the smooth muscle isoforms and the RLC binding site. The expressed short human aorta smooth muscle myosin construct resembles chymotryptic skeletal myosin subfragment 1 (S1) in its length, monomeric associative state, and content of one light chain (essential LC_{17a}). Lacking RLC, this smooth muscle myosin is persistently ''switched on'' for actin

Submitted November 9, 2006, and accepted for publication July 25, 2007.

Address reprint requests to Thomas P. Burghardt, E-mail: burghardt@mayo.edu.

Abbreviations used: CD, circular dichroism; Dc, *Dictyostelium discoideum*; DOPE, discrete optimized protein energy; ELC, essential light chain of myosin; k_{ET}, electron transfer rate; K_{SV}, Stern-Volmer quenching constant; MHC, myosin heavy chain; MYH11, human smooth muscle myosin 11 heavy-chain gene; MYL6, human smooth muscle myosin light-chain 6 gene; NATA, *N*-acetyl-L-tryptophanamide; NST, nucleotide sensitive tryptophan; S1, myosin subfragment 1; SH1(2), myosin reactive thiols; smS1A, smooth muscle myosin subfragment 1 containing ELC and lacking the seven-amino-acid active site insert; smS1B, smooth muscle myosin subfragment 1 containing ELC and containing the seven-amino-acid active site insert; W506F, W506 replacement with phenylalanine in smS1A; W506+, single tryptophan at AA506 construct from smS1A; W506+(Y499F), Y499F construct from W506+; WT, wild-type. Sequence numbering from human smooth muscle myosin isoform A.

Editor: Leepo C. Yu.

0006-3495/07/11/3555/12 $2.00

doi: 10.1529/biophysj.106.100818

activation. The protein also lacks the seven-amino-acid active site insert. We indicate our construct by smS1A.

The myosin ATPase cycle has intermediates maintaining unique NST fluorescence intensity levels providing an empirical tool for characterizing kinetics that was exploited to elucidate the myosin ATPase cycle (11,12). This cycle, summarized by the following scheme,

$$M + ATP \leftrightarrow M^{*}.ATP \leftrightarrow M^{**}.ADP.Pi \leftrightarrow M^{\wedge}.ADP + Pi \leftrightarrow M + ADP + Pi, \quad \text{(Scheme 1)}$$

has intermediates M, M*, M**, and M^ corresponding to the distinct myosin conformations. Work production occurs during hydrolysis product release when the active site ''back door'' opens to release product (13) and the motor lever arm rotates to impel attached actin (14). In steady state, the transient intermediates are occupied at fractional concentrations that are known for a variety of myosins (12,15,16). Nucleotide analogs induce static S1 structures imitating the transient intermediate conformations permitting their investigation with low time resolution techniques such as x-ray crystallography, CD, or steady-state fluorescence. Exhaustive study of the association of analog-induced and transient intermediate S1 structures lead to the identification of bound ATPγS or trapped ADP.BeF_x (low ionic strength) with M*.ATP, trapped ADP.Vi or ADP.AlF_4^- or ADP.BeF_x (high ionic strength) with M**.ADP.P_i, and bound ADP with M^.ADP (17–26).

Absorption dipole strength (27) and fluorescence intensity (28) increases are the consistently unequivocal response of the highly conserved W506 in the myosin motor to nucleotide binding and hydrolysis in the active site. This response has been recorded in skeletal, cardiac, smooth muscle (15), Dictyostelium discoideum (Dc) myosin II (29), and probably other myosin isoforms implying it results from a common structural origin within the function conserving motor. Early work ruled out a tryptophan residue located at the nucleotide binding site as the NST (30). The NST's identity was later suggested to be W506 on the basis of circular dichroism and fluorescence experiments identifying the peptide in myosin mobilized by ATP binding (31), Forster energy transfer between a probe modifying a reactive thiol (SH2) and tryptophan residues (32), by selective chemical modification of tryptophans (33), and by W506 emission isolation using difference spectroscopy between native myosin and a reactive thiol (SH1) modified version where W506 is selectively quenched (34,35). Much of the early work on the NST utilized tissue purified skeletal muscle myosin. Expressed myosins from Dc (29) and smooth muscle (36) elegantly confirmed NST identity as W506 and measured homologous NST properties in these divergent myosin II systems.

The notion of a common structural origin for Scheme 1 myosin energy transduction and NST fluorescence intensity modulation has motivated continued interest in W506 photophysics. Observation of NST dipole strength enhancement upon nucleotide binding and hydrolysis in the active site indicates at once that the effect perturbs the NST ground state (37) normally suggesting significant structural change. The accompanying NST fluorescence enhancement opens the possibility for excited state processes usually involving electron transfer (38,39) and/or solvent accessibility (40). Yoshino et al. (41) suggested a direct interaction between nucleotide and the NST indole as the mechanism for absorption enhancement in myosin that apparently conflicts with modern myosin crystal structures unavailable at the time. Bivin et al. (42) studied fluorescence from model diketopiperazines incorporating tryptophan and various charged residues and suggested local charged side chains modulate emission from the W506 indole without a measurable ground state effect. A Dc myosin motor domain mutant containing one tryptophan at position 506 suggested both ground and excited state mechanisms were in play (43). Tissue purified skeletal myosin S1 containing five tryptophans was studied with differential spectroscopy to isolate W506 absorption and emission. The fluorescence lifetimes and decay amplitudes indicated that W506 forms a ground-state complex with a static quencher inducing hypochromism in the tryptophan absorption band. The highly conserved tyrosine, Y499, was suggested as a likely static quencher (44,45).

Because WT smS1A has nucleotide-induced tryptophan fluorescence enhancement like other myosin isoforms we constructed three smS1A mutants to probe its structural basis. A tryptophan lite mutant, W506+, contains a single tryptophan at position 506. A knockout mutant, W506F, has phenylalanine at position 506 but retains the other six tryptophans from the native protein. A mutant of W506+, W506+(Y499F), has the conserved Y499 replaced with phenylalanine. W506+ lacks nucleotide sensitive fluorescence enhancement probably eliminating W506 as the NST. W506+(Y499F) has partially rescued enhancement demonstrating Y499's ability to induce nucleotide sensitivity in W506 as predicted (44,45). W506F retains nucleotide sensitive fluorescence enhancement despite significant perturbation of ATPase functionality. W506+(Y499F) also shows a perturbed ATPase functionality common for side-chain modifications in the vicinity of W506 (46,47).

Experimental results presented here, together with previous observations of NST fluorescence enhancement in smB isoforms, suggests that the smA and smB smooth muscle myosin isoforms differ in how influences propagate from the active site. The effect is apparent in the ability of W506 to sense ATP hydrolysis only in the smB isoform. The seven-amino-acid deletion from loop 1 in smA was previously implicated in altered ATPase kinetics attributed to local interference of the small loop 1 with ADP release. We demonstrate here that the shortened loop 1 also affects distant sites in the protein by measurably altering how information propagates from the active site. W506 sensitivity to nucleotide binding and hydrolysis is observed in many myosin isoforms

leading to its association with a conserved transduction mechanism in the motor. The present results open the possibility that smA could differ from other isoforms in its transduction mechanism.

METHODS

Chemicals

Ammonium sulfate, ATP, ADP, Na-Azide, dimethylformamide (DMF), dithiothreitol (DTT), phenylmethylsulfonyl fluoride (PMSF), *N*-acetyl-L-tryptophanamide (NATA), and β-D(+) glucose are from Sigma (St. Louis, MO). Phalloidin and pyrene iodoacetamide are from Molecular Probes (Eugene, OR). Bradford protein concentration assay is from Bio-Rad (Hercules, CA). Leupeptin, chymostatin, and pepstatin are from Roche Applied Sciences (Indianapolis, IN). Ni-NTA agarose was from Qiagen (Valencia, CA). Hexokinase is from Worthington Biochemical (Lakewood, NJ). All chemicals are reagent grade or Ultra-Pure if available.

Cloning of human myosin heavy chain (MYH11) and essential light chain (MYL6)

A potential full-length EST clone encoding MYH11 in *Sal*I/*Not*I pCMV-Sport 6 was obtained from American Type Culture Collection (ATCC) (No. 5182236). The clone was found to encode the entire catalytic and light-chain binding domains of MYH11 smA variant, but was lacking the C-terminal half of MYH11 due to truncation at an endogenous *Not*I site. The portion of the clone encoding the catalytic and essential light-chain binding regions (residues Met-1–Leu-813) was amplified by polymerase chain reaction (PCR). A Kozak consensus sequence was incorporated into the forward primer, and a 6× His encoding (plus stop codon) extension to immediately follow Leu-813 was included on the reverse primer. A full-length clone encoding human MYL6 isoform 1 in *Not*I/*Xho*I pBluescriptSK− was obtained from ATCC (No. 9322841). The full-length MYL6 isoform I was amplified by PCR with a Kozak consensus sequence included in the forward primer. Both PCR reactions were cloned into pCRBluntII Topo (Invitrogen, Carlsbad, CA) and sequenced in their entirety.

Site-directed mutagenesis

We sequentially mutated six of the seven endogenous tryptophans in pCRBluntII to phenylalanine or methionine using QuikChange Mutagenesis (Stratagene, La Jolla, CA) to produce a mutant heavy chain 813 residues long and containing a single tryptophan residue at position 506, W506+. In the W506+ construct, W33, W37, W435, W591, and W619 were changed to phenylalanine whereas W540 was changed to methionine. In the W506F single-site mutant construct, W506 was changed to phenylalanine. Finally, W506+(Y499F) was created from W506+ with Y499 changed to phenylalanine. Primers are listed in Table 1. The wild-type MYL6 (ELC), MYH11(1-813), and three mutated MYH11(1-813) constructs were subcloned into vector pVL1392 (Invitrogen). The accuracy of all constructs was verified by DNA sequencing.

Protein expression and purification

The baculovirus system was used to express wild-type and mutant constructs by coinfecting Sf9 insect cells with a recombinant baculovirus encoding WT-MYH11(1-813), W506+, W506F, or W506+(Y499F) and with a baculovirus encoding the wild-type MYL6 (ELC). Equal titers of the heavy and light chain encoded baculoviruses coinfected the Sf9 cells. Baculoviruses were prepared for protein expression using the Bac-to-Bac system (Invitrogen). Baculovirus stocks for heavy-chain and light-chain constructs were made at Mayo or the Tissue Culture Core Facility, University of Colorado Cancer Center, UCHSC at Fitzsimons, Aurora, CO. Protein expressions were carried out at both facilities.

TABLE 1 Primers for generating MYH11 mutants

Primer	Sequence (5′–3′)
W30F & W37F	CCCAGTGGCCCAGGCTGACTTTGCCGCCAAGA-GACTCGTCTTTGTCCCCTCGG
W435F	ATATGAGCGCCTTTTCCGCTTTATACTCACCC
W540M	GCTGGACGAGGAATGCATGTTCCCCAAAGCC
W591F	GACTATAATGCGAGTGCCTTTCTGACCAAGAA-TATGGACC
W619F	GTTTGTGGCCGACCTGTTTAAGGACGTGGACC-GCATCGTG
W506F	GAGGGCATCGAGTTCAACTTCATCGAC
Y499F	CATCCTGGAGCAGGAGGAGTTCCAGCGCGAG-GGCATCGAG

Wild-type and mutant proteins were purified as described by Onishi et al. (46) with modifications. Sf9 cells were lysed with hypotonic lysis buffer (20 mM Tris-HCl, pH 8.0, 4 mM $MgCl_2$, 5 mM DTT, 1 mM PMSF, 1 mM EGTA, 0.05 mg/ml leupeptin, 0.01 mg/ml chymostatin, and 0.01 mg/ml pepstatin). To extract S1 protein, NaCl was added to 0.3 M and ATP was added to 2 mM. The extract was fractionated with 34% and 70% ammonium sulfate and then dialyzed for 4 h against 20 mM Tris-HCl, pH 7.5, 2 mM $MgCl_2$, 4 mM DTT, 0.2 mM PMSF, 0.2 M KCl, and 0.01 mg/ml leupeptin. The dialyzed sample was incubated with 10% glucose and 20 units/ml of hexokinase to remove residual ATP and then mixed with phalloidin stabilized F-actin for 2 h at 4°C. The actoS1 complex was collected via centrifugation and dialyzed overnight against 20 mM Tris-HCl, pH 7.5, 2 mM $MgCl_2$, 7 mM 2-mercaptoethanol, 0.5 mM PMSF, 0.2 M KCl, 0.01 mg/ml leupeptin, and 1 mM ATP. The actin was then dissociated from the S1 by adding another 1 mM ATP. His-tagged S1 was further purified using Ni-NTA agarose. On average, 1–2 mg of protein was purified from 1×10^9 cells. Protein purity ranged from 90 to 98%. Expressed protein samples are shown in Fig. 1 using 12% SDS-PAGE. The eluted sample was treated with 5 mM EDTA to remove residual bound nucleotide and precipitated in a dialysis solution of 25 mM TES, pH 7.0, 1 mM EDTA, 1 mM DTT, and 1 μg/ml leupeptin containing 75% ammonium sulfate. The precipitate was collected via centrifugation and stored at −20°C for 2–3 months with no loss of specific activity.

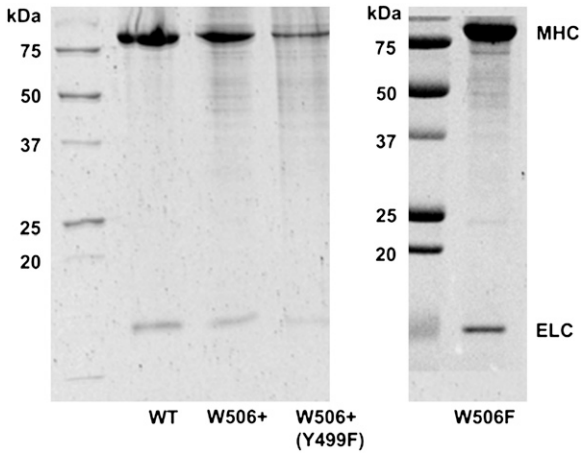

FIGURE 1 Purified expressed WT, W506+, W506+(Y499F), and W506F constructs containing MHC and ELC are shown as are standard molecular weight proteins in 12% SDS-PAGE.

Rabbit skeletal chymotryptic S1 was prepared according to Weeds and Taylor (48). Skeletal actin was prepared from rabbit skeletal muscle acetone dried powder according to Pardee and Spudich (49).

Protein concentration was estimated by using the Bradford assay with bovine serum albumin as protein standard. Molecular mass was assumed to the 115 kDa for smS1A.

Expressed protein sequencing by mass spectrometry

Colloidal blue stained SDS-PAGE gel bands were reduced and alkylated with DTT and iodoacetamide then digested with either endoproteinase Lys-C (Wako Chemicals, Richmond, VA) or endoproteinase Asp-N (Roche Applied Science, Indianapolis, IN). Extracted peptides were analyzed by nano-flow liquid chromatography tandem mass spectrometry (nanoLC-MS/MS) using a ThermoFinnigan LTQ Orbitrap Hybrid Mass Spectrometer (50) (ThermoElectron, Bremen, Germany) coupled to an Eksigent nanoLC-2D HPLC system (Eksigent, Dublin, CA). The MS/MS raw data were searched using SEQUEST (51) in ThermoElectron Bioworks 3.2 to correlate the observed MS/MS fragment ions to theoretical fragment ions of all peptides from the expected myosin mutated sequences. Searches were conducted with fixed cysteine modifications of +57 for carboxamidomethyl-cysteines and variable modifications allowing +16 with methionines for methione sulphoxide. Peptide mass search tolerances were set to 20 ppm and fragment mass tolerance set to ±1.0 Da. The search was performed without specifying an enzyme to confirm that the acceptable high scoring peptides corresponded to the appropriate Asp-N or Lys-C cleavage sites. All mutated peptide matches gave Sequest Xcorr values >2.5 for $z = 2$ precursor ions and were within 1 ppm of the expected masses. The fragment ion matches were manually inspected. The digests were also searched against the Swissprotein database using the appropriate enzyme, with the same parameters to note the matches from the wild-type sequence. No wild-type versions of the mutated sequences were observed.

The mass spectrometry results confirmed peptide sequences for W506+ and W506+(Y499F) mutant heavy-chain constructs. Mass spectrometry was not performed on W506F.

ATPase and actin-activated ATPase assays

K^+EDTA-ATPase activity was measured on samples at 37°C in 250 μl aliquots containing 0.35–0.70 μM expressed smS1A, 0.6 M KCl, 10 mM EDTA, 25 mM Tris-HCl, pH 8.0, with 2 mM ATP. The Ca^{2+}ATPase assay test solution was identical to that of K^+EDTA-ATPase except 10 mM $CaCl_2$ replaced the EDTA. Inorganic phosphate production from the ATPase reaction was measured using the Fiske-Subbarow method (52).

Mg^{2+}ATPase and actin-activated Mg^{2+}ATPase activities were measured at 25°C in 220 μl aliquots containing 1 μM expressed smS1A, 60 mM KCl, 4 mM $MgCl_2$, 1 mM EGTA, 1 mM DTT, 25 mM Tris-HCl, pH 7.6, with 1 mM ATP. Curves of Mg^{2+} ATPase versus actin concentration, [A], were evaluated with the equation $V = V_{max}/(1 + K_M/[A])$ to obtain the apparent dissociation constant and maximum velocity, K_M and V_{max}. Baseline Mg^{2+}ATPase activity at $[A] = 0$ was subtracted from all data points. Inorganic phosphate production from the ATPase reaction was measured using the malachite green assay (53).

Pyrene labeled actin experiments

The actin binding assay used phalloidin stabilized pyrene iodoacetamide labeled actin (54,55,55). Labeling efficiency was 96%. Myosin binding was assessed using 0.2 μM actin in rigor or in the presence of 0.5 mM MgADP as described previously (55–58). The ADP stock solution was pretreated with 35 units hexokinase and 10% glucose to remove ATP impurities. Measurements were done at 20°C in 20 mM TES, pH 7.2, 0.1 M KCl, 2 mM $MgCl_2$, 1 mM DTT, and 1 μg/ml leupeptin. Binding constants were surmised from myosin titration curves as described by Conibear and Geeves (56). Reversibility of the actin binding was measured by adding 8 mM ATP to the sample after completing the binding measurements; 85–90% of pyrene fluorescence intensity was recovered after ATP addition.

Spectroscopy measurements

Measuring buffer consisted of 0.45 M KCl, 20 mM Tris-HCl, pH 7.5, 2 mM $MgCl_2$, and 0.5 mM DTT. ADP or ATP bound states of WT, W506+, W506+(Y499F), and W506F were formed by incubating the proteins at concentrations of 0.8–8.0 μM in measuring buffer with 0.133 mM ADP or 0.1 mM ATP for 3 min at 20°C. Apo-protein was treated identically but without addition of nucleotide.

Trapped nucleotide analogs of smS1A were formed by incubating the proteins at concentrations of 0.8–8.0 μM in measuring buffer with 5 mM KF and 0.133 mM ADP for 3 min at 20°C. $BeCl_2$ (0.2 mM) or $AlCl_3$ (0.2 mM) were added and incubated at the same temperature for 30 min forming ADP.BeF_x-smS1A and ADP.AlF_4^--smS1A trapped complexes. Efficient trapping of W506+(Y499F) and W506F required use of 10 mM KF and 0.5 mM $AlCl_3$. Stable complex formation was tested by measuring inhibition of K^+EDTA ATPase activity. Ca^{2+}ATPase was used to assess active site trapping in W506+(Y499F) and W506F because these mutants have no K^+EDTA ATPase. Trapped smS1A had >90% ATPase inhibition.

Absorption spectra were measured on a Beckman DU650 (Beckman Coulter, Fullerton, CA) or Cary 5E (Varian, Palo Alto, CA) at room temperature. Differential protein absorption measurements detecting small changes in tryptophan extinction were carried out on the Cary in 3-mm pathlength rectangular cells and utilizing Apo or trapped ADP.AlF_4^- protein at 2–4 μM concentration.

Circular dichroism (CD) spectra were recorded on a JASCO J715 at 8°C following the procedure described previously (59). The measurements were carried out in 1–2 mm pathlength cells on Apo-protein at 6–8 μM concentration. CD spectra are plotted as extinction, $\Delta\varepsilon$ (60).

Steady-state and time-resolved tryptophan fluorescence measurements were performed with a PTI QuantaMaster spectrofluorometer (PTI, London, Ontario, Canada) at 20°C. Measurements were carried out in a 3-mm pathlength rectangular cell on protein samples with optical density ~0.05 (~0.12 μM protein and ~0.13 mM nucleotide) for all wavelengths studied. Protein samples included Apo, ADP or ATP bound, and, ADP.BeF_x or ADP.AlF_4^- trapped smS1A. Samples were illuminated with 298-nm wavelength light suitable for selective excitation of tryptophan. Steady-state measurements used an excitation bandwidth of 2 nm with emission collected through a band-pass filter centered at 342 ± 5 nm. Time-resolved measurements were conducted using analog fluorescence lifetime detection and pulsed laser excitation. The 337–nm line from a pulsed nitrogen laser pumps a dye laser containing rhodamine 590 (Exciton, Dayton, OH) with output frequency-doubled to give 298-nm wavelength light. Emission was detected at 340 nm with monochromator bandwidth of 8 nm.

The excitation pulse convoluted with detector response, the instrument response function, is ~1.3 ns fullwidth at half-maximum. Observed time-resolved fluorescence intensity was fitted by convoluting the instrument response function with an exponential fitting function,

$$F(t) = \sum_{i=1}^{p} A_i e^{-t/\tau_i} \quad (1)$$

where A_i is the decay amplitude and τ_i the lifetime for the i^{th} component (61). Best fits were located using a nonlinear least-squares protocol.

We observed *N*-acetyl-L-tryptophanamide (NATA) to have a single 3.5-ns lifetime in 0.1 M sodium phosphate pH 7 at 20°C. The value obtained with our instrument is somewhat longer than the 3.0-ns lifetime observed previously (62). We verified that protein rotational relaxation does not make a significant contribution to fluorescence intensity relaxation as shown previously (44).

Dynamic quenching of W506 steady-state fluorescence, F, is heterogeneous with quencher accessible and inaccessible components. The Lehrer equation,

$$\frac{F_0}{F_0 - F} = \frac{1}{fK_{SV}[Q]} + \frac{1}{f} \quad (2)$$

is appropriate for this case where F_0 is fluorescence intensity in the absence of quencher, K_{SV} is the Stern-Volmer constant for the accessible component, $[Q]$ the quencher concentration, and f the fraction of total fluorescence intensity accessible to Q (40). Acrylamide quenching data is used to estimate K_{SV} and f by linear least-squares fitting.

Steady-state pyrene-actin fluorescence measurements were also performed with the PTI spectrofluorometer. Samples were illuminated with 365-nm light and emission collected through a band-pass filter centered at 402 ± 5 nm. Excitation monochromator bandwidth was 2 nm.

Homology modeling

Homology modeling was done with Modeller 8.2 (63) on the myosin heavy chain (MHC) and ELC. Smooth muscle and skeletal myosin atomic structures 1br1 (23) and 2mys (64) were the templates for the M** and M conformations (see Scheme 1). Target sequences, consisting of the first 812 residues from MHC (sequence identifier gi13124879) and all 149 residues from ELC (gi17986258) from the MYH11 gene, included both WT and mutant sequences. Skeletal and smooth muscle MHC (gi13432175 and gi3915778) and ELC (gi1942540 and gi5542589) targets were likewise folded into the M and M** template for assessing modeling accuracy.

Homology model accuracy was evaluated using the DOPE score as suggested in the Modeller 8.2 tutorial. The DOPE score is proportional to potential energy per residue, smoothed over a 15-residue window, and normalized by the number of restraints acting on each residue. It indicates problem regions in the homology model when profiles are compared from target and template sequences. Supplementary Fig. S1 *A* (see Supplementary Material) compares DOPE profiles for skeletal, WT, and W506+ sequences consisting of 961 residues from truncated MHC and ELC used in this study and folded with the 2mys template. The skeletal sequence folded into the skeletal template produces a DOPE profile comparable to those for the MYH11 sequences folded into the skeletal template for the entire peptide suggesting MYH11 sequences are accurately folded. Supplementary Fig. S1 *B* (see Supplementary Material) shows results for the 1br1 template. The latter has a higher sequence identity with MYH11 and more favorable DOPE profiles for the native and mutant sequences. The single notable DOPE score anomaly occurs with the skeletal template at AA525-527 (supplementary Fig. S1 *A*) where smooth muscle myosin isoforms have a Pro-Asn-Asn insert producing a kink in the switch II helix. The DOPE score at this position is also elevated for the smooth muscle myosin template (supplementary Fig. S1 *B*) suggesting it is an intrinsic property of the sequence rather than a poorly folded kink.

RESULTS

Myosin and actin-activated myosin ATPase

K^+EDTA, Ca^{2+}, and Mg^{2+} ATPases for the WT and mutant smS1As are compared in Table 2. WT and W506+ K^+EDTA, Ca^{2+}, and Mg^{2+} ATPases are comparable but slightly inhibited in the mutant indicating undisturbed functional performance in these tests. K^+EDTA or Mg^{2+} ATPases are ~95% inhibited or dramatically enhanced for W506F and W506+(Y499F) compared to WT. Ca^{2+} ATPase is dramatically enhanced in the W506F mutant compared to WT. Mg^{2+} ATPase enhancement in W506+(Y499F) is identical to that from actin activation of the WT protein. Similar changes to the ATPases were observed for the smB isoform with the W506F replacement (46) and in skeletal myosin with covalent modification of SH1 (65). W506, Y499, and SH1 occupy the interface of the switch II helix (W506 and Y499) and converter domain (SH1) where significant conformation change occurs during energy transduction. The residues are probably related by their common occupation of a propagating conformation change pathway emanating from the myosin active site (66) and by sensitivity to lever arm movement.

Fig. 2 shows actin-activated Mg^{2+}ATPase data for WT (*solid square*), W506+ (*solid uptriangle*), and W506+(Y499F) (*solid diamond*) proteins. Table 2 summarizes K_M and V_{max} computed from these data. V_{max} decreases approximately threefold, whereas K_M is identical, for W506+ compared to WT. The W506+(Y499F) mutant Mg^{2+} ATPase was not actin activated. These results parallel those observed for the WT and mutant smB isoform (36,46).

Actin binding

Strong actin binding to smS1A was measured using phalloidin stabilized, pyrene-labeled actin assay. Fig. 3 shows pyrene-actin fluorescence versus myosin head concentration for W506+ in the Apo and ADP bound states. Fitted curves provide the actomyosin binding constant. Binding constants are listed in Table 3 for Apo and ADP states of WT, W506+, and W506+(Y499F). All the smS1A binding constants are

TABLE 2 Myosin ATPases

	ATPase (s^{-1})			Actin-activated Mg^{2+} ATPase	
Isoform	K^+EDTA	Ca^{2+}	Mg^{2+}	V_{max} (s^{-1})	K_M (μM)
WT	3.5 ± 0.2	2.4 ± 0.3	0.04 ± 0.02	0.20 ± 0.03	85.1 ± 25.7
W506+	2.6 ± 0.2	1.5 ± 0.5	0.023 ± 0.003	0.06 ± 0.01	66.5 ± 29.8
W506+(Y499F)	0.16 ± 0.04	2.8 ± 0.4	0.22 ± 0.01	NA*	NA*
W506F	0.18 ± 0.01	9.5 ± 0.4	0.41 ± 0.01	NM†	NM†

All uncertainties are mean ± SE for $n \geq 3$.
*Not activated.
†Not measured.

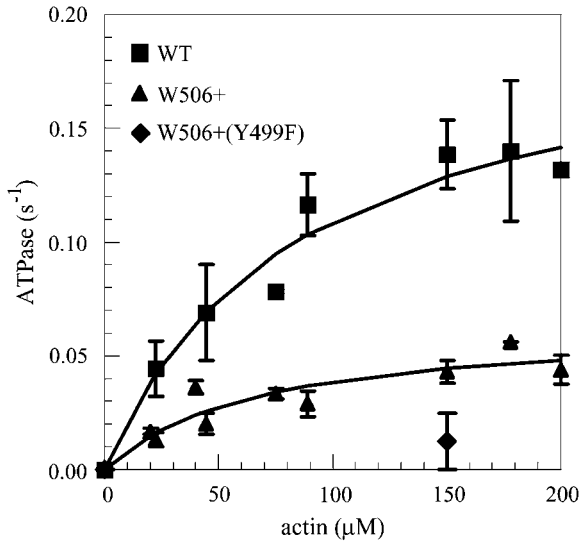

FIGURE 2 Actin-activated Mg^{2+}ATPase for the WT (■), W506+ (▲), and W506+(Y499F) (♦) smA proteins. Error bars indicate mean ± SE for $n \geq 3$. Dissociation constant, K_M, and maximum ATPase velocity, V_{max}, tabulated from the data using $V = V_{max}/(1 + K_M/[A])$ are listed in Table 2.

larger than the rabbit Apo S1 binding constant of ~10 $(\mu M)^{-1}$ and fall into the order $K_{Apo}(WT) \gg K_{Apo}(W506+) > K_{Apo}[W506+(Y499F)]$. The picture is similar for the ADP state with $K_{ADP}(WT) > K_{ADP}(W506+) \gg K_{ADP}[W506+(Y499F)]$ suggesting that the accumulated mutations weaken strong actin binding. ADP decreases affinity for actin in the WT and mutant forms by two- to fourfold. Similar modest

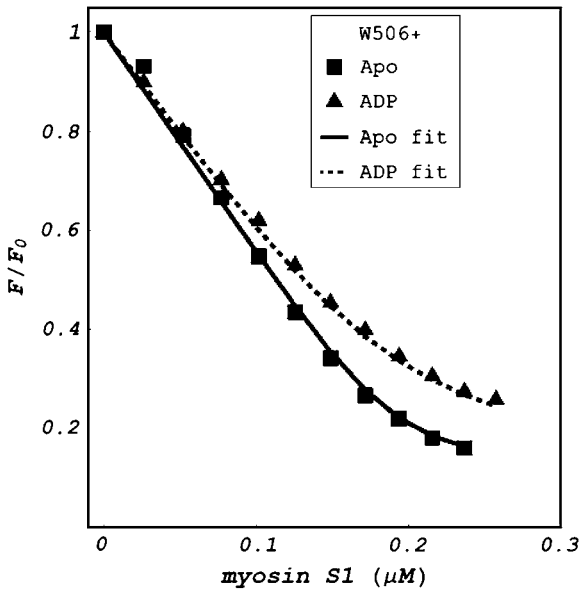

FIGURE 3 Normalized pyrene labeled actin fluorescence versus myosin head concentration for W506+ in the Apo and ADP bound states. Fitted curves provide the actomyosin binding constant. Binding constants are listed in Table 3 for Apo and ADP states of WT, W506+, and W506+(Y499F).

TABLE 3 WT and mutant smS1A equilibrium actin binding constants

	$K\ (\mu M)^{-1}$	
Isoform	Apo	ADP
WT	165 ± 30	74 ± 15
W506+	192 ± 40	42 ± 5
W506+(Y499F)	56 ± 15	30 ± 5

M+A↔M.A and $K = [M.A]/([M][A])$, for M and A myosin and actin, are the binding scheme and equilibrium binding constant used to analyze data. All uncertainties are mean ± SE for $n = 5$.

decreases (approximately twofold) in actin binding affinity due to ADP were observed for nonmuscle cytoplasmic myosin IIA (67) in contrast to the 5- to 60-fold decrease for smB, cardiac, and skeletal myosin (68,69). Actin-activated ATPase (Fig. 2 and Table 2) indicated actin binding in the presence of ATP is identical for WT and W506+.

WT and mutant smS1A absorption and circular dichroism spectroscopy

Fig. 4 (*A*) shows the steady-state extinction coefficient spectrum, ε, from WT, W506+, and W506+(Y499F). Six excess tryptophans in the WT protein shift extinction maximum to the red as expected. Below 280 nm the tyrosine side-chain absorption dominates. Tryptophan induced hypochromism in the tyrosine contribution to the spectrum probably causes the WT to fall below the W506+ spectrum despite their identical tyrosine content. Alternatively, structural change induced by the tryptophan substitutions in W506+ might cause an increase in tyrosine extinction. The W506+(Y499F) extinction spectrum detects the deletion of the tyrosine at AA499 with a slight decrease in extinction compared to W506+ below ~280 nm.

Fig. 4 (*B*) is the difference extinction spectrum for the M** and M conformations in WT, W506+, and W506+(Y499F). The M** conformation was induced by active site trapping with ADP.AlF_4^-. The data show that the absorption dipole moment increases for the M** conformation compared to the Apo form in the order WT > W506+(Y499F) > W506+. The enhancement is quantitatively similar to observations from native skeletal S1 (27,44) indicating nucleotide binding and hydrolysis similarly perturbs W506 ground state interactions in the two isoforms. The W506+ mutant has about half the enhancement of the WT whereas the W506+(Y499F) mutant is intermediate.

Fig. 4 (*C*) shows the steady-state CD extinction coefficient spectrum, $\Delta\varepsilon$, from rabbit S1, WT, W506+, and W506+(Y499F). Tryptophan near ultraviolet CD is uniquely detected at wavelengths >295 nm. The rabbit S1 has a peak at 295 nm that is suppressed in the WT-smS1A despite the six tryptophan residues present (compared to five in the chymotryptic rabbit S1). Similar CD in the tryptophan spectral region for the smA isoforms diverge at shorter wavelengths where both tyrosine and tryptophan absorb.

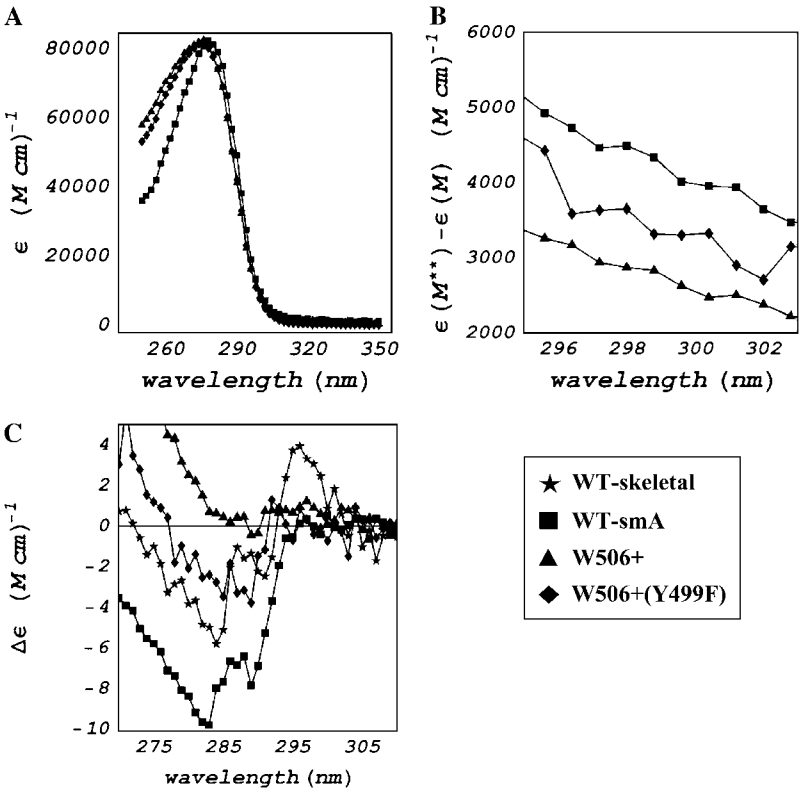

FIGURE 4 Spectra for smS1A WT, W506+, W506+ (Y499F), and rabbit skeletal S1. (*A*) Extinction coefficient spectra, ε. (*B*) Extinction spectrum change upon active site trapping with ADP.AlF_4^-. (*C*) CD extinction spectra, $\Delta\varepsilon$.

WT and mutant smS1A fluorescence spectroscopy

Steady-state and time-resolved fluorescence measurements performed on the WT and mutant isoforms of the smS1A investigated the effect of active site conformation on W506 fluorescence intensity. Fig. 5 compares steady-state fluorescence intensity increment, $\Delta I = [F(\text{nucleotide/analog}) - F(\text{Apo})]/F(\text{Apo})$, for ATP, ADP, and the trapped analogs ADP.BeF_x and ADP.AlF_4^-. We find that the incremental fluorescence response of W506 to active site conformation in W506+ is negligible. The data show that it is improbable that the highly conserved W506 is responsible for the WT intensity increment unlike in the skeletal and smB myosins (15,29). In contrast, Y499F replacement in W506+ sensitizes W506 to nucleotide whereas W506F produces a modest nucleotide-induced increment.

The highly conserved Y499 plays a role in how W506 responds to active site occupancy. In W506+ and W506+ (Y499F), W506 undergoes nucleotide-induced extinction increase (Fig. 4 *B*) that is reduced by Y499. Thus the Y499 side chain affects W506 ground state to minimize (but not eliminate) nucleotide-induced extinction enhancement. Y499 further reduces fluorescence enhancement by excited state quenching to give no net fluorescence increment in W506+. In other myosin isoforms, where changing active site conformation significantly modulates W506 intensity, Y499 is probably involved similarly except that the net effect is W506 fluorescence enhancement. Changing Y499 from a nucleotide-induced net excited state quencher of W506 fluorescence in smA to a net excited state enhancer of W506 fluorescence in smB could be accomplished with a minor relative side-chain conformation adjustment between W506 and Y499 much smaller than one probably imposed by

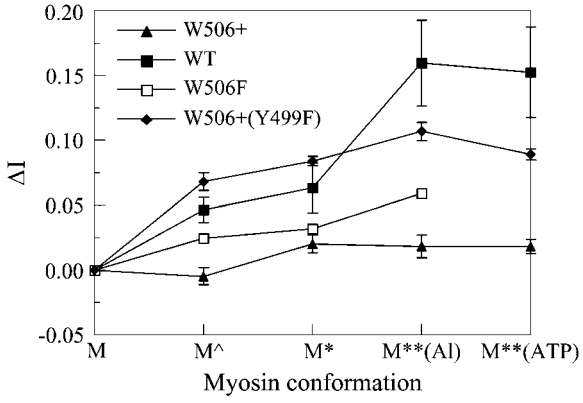

FIGURE 5 The fluorescence intensity increment, $\Delta I = (F(\text{nucleotide/analog}) - F(\text{Apo}))/F(\text{Apo})$, for ATP, ADP (M^), and trapped nucleotide analogs ADP.BeF_x (M*) and ADP.AlF_4^-. The WT (■), W506+ (▲), W506+(Y499F) (♦), and W506F (□) isoforms are depicted. The ATP induced M** conformation was not observed with the W506F construct because its high Mg^{2+} ATPase prohibits the system from reaching steady state with a predominant M** conformation. Error bars indicate mean SE for $n \geq 9$ ($\geq$7 for W506F). For W506F error bars are smaller than the size of the open square symbol.

primary sequence variation between the two isoforms. Simulations reported previously for the skeletal isoform suggest Y499 is the only side-chain group significantly modulating W506 fluorescence intensity by ground state interaction (44). Backbone carbonyl groups are an important tryptophan fluorescence quencher in peptides (38) and are likely additional important contributors to W506 intensity modulation.

The W506F nucleotide-induced fluorescence enhancement agrees qualitatively with the lack of enhancement in the W506+ species. Quantitatively, W506F enhancement is below that observed in WT. This finding is expected since the homologous mutation in the Dc myosin II motor domain shows the construct does not form the high enhancement M** species in the presence of ATP (70). Thus the enhancement equivalence in WT M* and ADP.AlF_4^- trapped W506F is due to the inability of W506F to form M**. A similar effect is seen in the W506+(Y499F) construct where nucleotide-induced fluorescence enhancements shown in Fig. 5 level off downstream of M*. Enhancements for ADP bound and ADP.BeF_x trapped W506F are also lower than in WT. Structural differences between W506F and WT that diminish tryptophan fluorescence enhancement in W506F is a possible rationalization. Significant structural differences between W506F or W506+(Y499F) on the one hand, and, WT or W506+ on the other are indicated by perturbed ATPases in the former (Table 2).

W506 fluorescence intensity decay in W506+ is characterized by two exponential functions $A_1\exp(-t/\tau_1) + A_2\exp(-t/\tau_2)$ (Eq. 1) with amplitudes and lifetimes summarized in Table 4 (top). Amplitudes are normalized by requiring $A_1\tau_1 + A_2\tau_2 = 1$ for that Apo conformation. Lifetimes fall into two groups containing the M and M^ (Apo and ADP) on the one hand and M* and M** (ADPBeF_x, ADPAlF_4^-, and ATP) conformations on the other. The latter conformations have slightly shorter lifetimes.

W506 fluorescence intensity decay in W506+(Y499F) is likewise characterized by two exponential functions with amplitudes and lifetimes summarized in Table 4 (bottom). Amplitudes are normalized like the W506+ mutant. Lifetimes again partition into two groups containing M and M^ (Apo and ADP) on the one hand and M* and M** (ADPBeF_x, ADPAlF_4^-, and ATP) on the other. In this case, M* and M** conformations have much longer lifetimes. The data is consistent with removal of an electron transfer partner from the vicinity of W506.

W506+ acrylamide quenching

Acrylamide is a dynamic quencher of solvent accessible tryptophans in myosin (34). Fig. 6 *A* shows the normalized steady-state fluorescence difference, $\Delta F = (F_0 - F)/F_0$ where F_0 is intensity without quencher, as a function of acrylamide concentration for W506+. The apparently saturable signal indicates W506 samples two environments, one accessible and another inaccessible to solution borne quencher. This is very different from skeletal muscle myosin and the smB isoform of smooth muscle myosin where W506 fluorescence does not have an inaccessible component (34,36). Fig. 6 *B* indicates $1/\Delta F$ for Apo and ATP bound W506+ vs. 1/[Q] where, according to Eq. 2, the *y*-intercept is $1/f$ and slope is $1/(fK_{SV})$. The data show the contrast between the states where ATP bound protein has a homogeneously accessible W506 whereas nearly half of the fluorescence is inaccessible in the Apo form. Table 5 summarizes Stern-Volmer constants and the accessible fluorescence fractions of W506 in the various myosin conformations. We see that in the M** conformation (ATP and ADP.AlF_4^-) all W506 fluorescence is accessible to acrylamide quenching. This fraction decreases significantly in the M and M* conformations with a minimum of ~0.6 in the M conformation. The Apo form of the protein has highly heterogeneous tryptophan fluorescence and a large Stern-Volmer quenching constant for the accessible portion of the tryptophan fluorescence. The ATP and ADP.AlF_4^- induced M** conformation is homogeneously accessible to tryptophan quenching with a small Stern-Volmer constant. The ADP.BeF_x induced

TABLE 4 W506+ and W506+(Y499F) time-resolved emission relaxation

		Lifetime		Amplitude	
Active site	Conformation	τ_1	τ_2	A_1	A_2
W506+					
Apo	M	0.89 ± 0.05	4.77 ± 0.08	0.10 ± 0.01	0.19 ± 0.01
ADP	M^	1.25 ± 0.24	4.89 ± 0.12	0.09 ± 0.01	0.18 ± 0.01
ADP.BeF_x	M*	0.48 ± 0.07	4.38 ± 0.05	0.18 ± 0.01	0.20 ± 0.01
ADP.AlF_4^-	M**	0.77 ± 0.08	4.63 ± 0.09	0.13 ± 0.01	0.19 ± 0.01
ATP	M**	0.51 ± 0.11	4.38 ± 0.09	0.14 ± 0.01	0.20 ± 0.01
W506+(Y499F)					
Apo	M	1.75 ± 0.04	5.26 ± 0.03	0.11 ± 0.02	0.15 ± 0.01
ADP	M^	0.98 ± 0.16	4.76 ± 0.14	0.13 ± 0.01	0.19 ± 0.02
ADP.BeF_x	M*	2.05 ± 0.02	6.13 ± 0.02	0.15 ± 0.02	0.12 ± 0.01
ADP.AlF_4^-	M**	2.34 ± 0.06	6.61 ± 0.14	0.21 ± 0.01	0.09 ± 0.01
ATP	M**	2.31 ± 0.07	6.32 ± 0.12	0.14 ± 0.03	0.11 ± 0.01

All uncertainties are mean ± SE for $n \geq 3$.

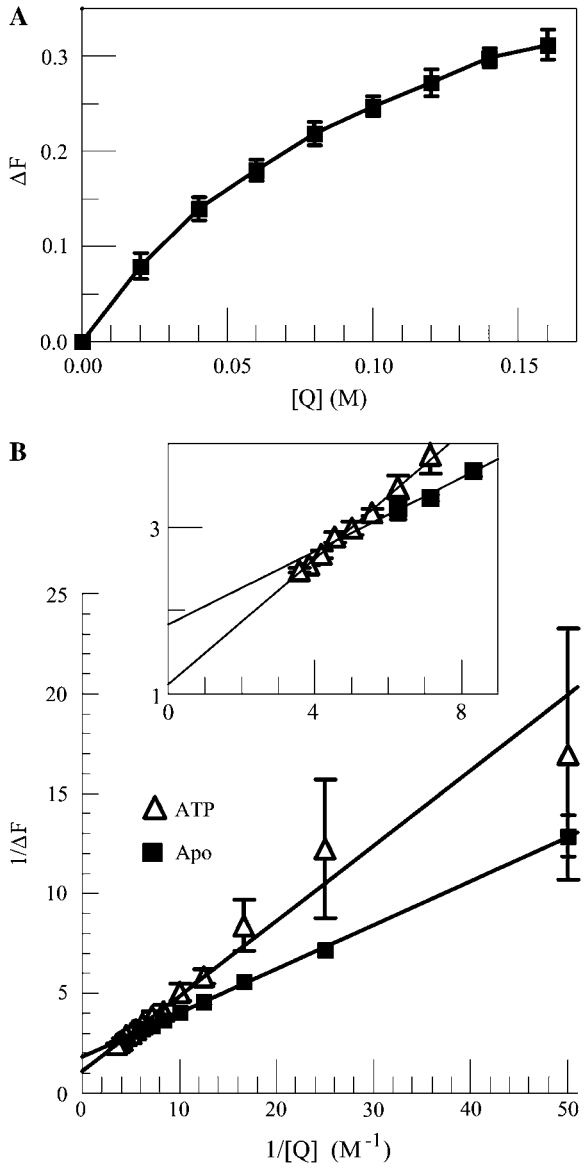

FIGURE 6 (*A*) Normalized steady-state fluorescence intensity difference, $\Delta F = (F_0 - F)/F_0$ where F_0 is intensity without quencher, as a function of acrylamide concentration, [Q], for W506+. Error bars indicate mean ± SE for $n = 4$. (*B*) Double reciprocal plot of acrylamide concentration versus ΔF (see Eq. 2) for Apo and ATP bound W506+. The slope of the fitted curves is $1/(f\ K_{SV})$ where f is the quencher accessible fraction and K_{SV} the Stern-Volmer constant. Insert is a close-up of the *y*-intercept equaling $1/f$. Error bars indicate mean ± SE for $n \geq 2$. Table 5 summarizes K_{SV} and f of W506+ in the various myosin conformations.

M* conformation has intermediate K_{SV} and accessible fraction.

Fluorescence lifetime data do not anticipate the heterogeneous acrylamide accessibility to W506. The shorter tryptophan fluorescence lifetime (Table 4) accounts for $\lesssim 10\%$ of the total emission intensity in all states hence the longer lifetime emits light from both environments detected by acrylamide quenching. We attempted to partition the longer lifetime component into two subcomponents but the curve fitting did not give interpretable results. Although acrylamide quenching readily distinguishes two probe environments in the majority fluorescence emission, W506 lifetimes in these two environments are not readily distinguished.

TABLE 5 Stern-Volmer constants and quenchable fluorescence fractions of W506+

Active site	Conformation	K_{SV}	f
Apo	M	8.9 ± 1.9	0.57 ± 0.07 (4)
ADP.BeF_x	M*	6.5 ± 1.3	0.67 ± 0.11 (3)
ADP.AlF_4^-	M**	4.8 ± 0.6	0.94 ± 0.21 (3)
ATP	M**	2.7 ± 1.3	1.14 ± 0.36 (2)

All uncertainties are mean ± SE for (*n*) experiments.

DISCUSSION

The protein matrix of atoms is a heterogeneous medium propagating structure deformations that perform functional time-ordered protein conformation change. In myosin, deformations are manifested as the ability of nucleotide binding and hydrolysis at the active site to remotely affect lever arm attitude and actin binding affinity. Causal active site control of remote sites follows from the observation that myosin converts ATP to products during contractile movement rather that contractile movement generating ATP from products. Hence, remote sites are linked by physical pathways through the protein matrix and by causality, the time ordering of dependent events. We study some of these elements of the transduction mechanism with experiments conducted on a human tonic smooth muscle myosin construct.

Human tonic and phasic smooth muscle myosins differ by a seven-amino-acid segment in loop 1 at the active site. The loop 1 shortened by the deleted segment in the tonic smA isoform alters myosin enzyme kinetics probably by inhibiting product egress or substrate ingress (5–7,67). Homology modeling of smA and smB isoforms confirms that loop 1 structural heterogeneity is reduced in smA implying the same for loop 1 flexibility. However, experimental results presented here argue that the differences induced by the seven-amino-acid deletion goes beyond steric inhibition of substrate to affect spatial aspects of propagating structure deformation in the motor core.

The chief experimental evidence for a difference in transduction mechanism between smA and smB is that the NST in all tested myosins is W506 except, as we have shown, for the human tonic smooth muscle myosin smA isoform. Absorption dipole strength and fluorescence intensity increases in the highly conserved W506 consistently accompany active site nucleotide binding and hydrolysis in a variety of myosin isoforms implying it results from a common structural origin within the conserved protein core (27–29,31–36). However, the tryptophan lite construct (W506+) containing one

tryptophan at position 506 has lowered nucleotide-induced dipole strength enhancement (Fig. 4) and no fluorescence enhancement (Fig. 5). Fluorescence lifetimes are also little affected by nucleotide in the active site (Table 4). W506 exposure to solution borne acrylamide changes measurably upon nucleotide binding and hydrolysis in the active site (Fig. 6) in a manner very different from that observed for skeletal (34) and smooth muscle smB myosin (36). The presence of a substantial acrylamide inaccessible fraction of W506 fluorescence, most pronounced in the apo-form of smS1A, was not seen previously. Control experiments assessed construct functionality by comparing with WT its myosin ATPase (Table 2), actin-activated myosin ATPase (Table 2), and strong binding to pyrene labeled actin (Fig. 3 and Table 3). W506+ shows nearly identical ATPase and K_M, but has an actin-activated ATPase $V_{max} \sim 1/3$ that of WT. Its strong binding to actin in Apo and ADP conformations is very similar to the WT. The W506+ to WT characteristics comparison parallels that of the homologous tryptophan lite construct in smB (36,46). We found W506+ to be completely functional by these metrics.

The highly conserved Y499 was predicted to affect W506 spectroscopy in skeletal S1 based on ground state calculations from static myosin crystal structures (35,44). The W506+(Y499F) mutant indicates Y499 affects W506 absorption (Fig. 4 *B*) and fluorescence (see the W506+(Y499) curve in Fig. 5). Data in Fig. 4 *B* imply interaction with Y499 diminishes nucleotide-induced extinction enhancement in W506 (extinction enhancement in W506 is larger without Y499). Data in Fig. 5 imply interaction with Y499 eliminates nucleotide-induced fluorescence enhancement in W506 (fluorescence enhancement in W506 is absent in the presence of Y499). These effects could be one in the same if diminished extinction is solely responsible for the lack of fluorescence enhancement in W506+ or could be independent with an excited state interaction between Y499 and W506 also needed to fully nullify enhancement. The latter is more likely because W506 (by Fig. 4 *B*) is nucleotide sensitive and an enhancement detectable with absorption is normally detectable by fluorescence. Since no fluorescence enhancement is observed (by Fig. 5), Y499 is probably quenching W506 by an excited state process. The latter is supported by the significantly longer W506 fluorescence lifetimes in W506+(Y499F) compared to W506+ for the M* and M** conformations (Table 4). We predicted the interaction between the skeletal myosin homologs of Y499 and W506, however, fluorescence enhancement in smA and skeletal myosin is obviously different and there are several possible explanations. For instance, i), the Y499/W506 ground state interaction enhancement is identical for both isoforms but Y499 is a suppressor (smA) or enhancer (skeletal) of W506 emission, ii), only differences in the Y499/W506 ground state interaction enhancement between isoforms give rise to the different nucleotide sensitivity, or iii), some combination of i and ii.

Reduced nucleotide-induced tryptophan fluorescence enhancement in the W506F construct compared to WT is most likely from the structural perturbation introduced by mutation making W506F unable to form the M** conformation as shown previously for the homologous mutation in the Dc myosin II motor domain (70). Both W506+(Y499F) and W506F constructs have elevated Mg^{2+} and Ca^{2+} ATPases and negligible K^+EDTA-ATPases compared to W506+ and WT. W506+(Y499F) binds actin less strongly in the Apo conformation compared to W506+ and WT and it is not actin activated. All changes in W506+(Y499F) and W506F functionality parallel changes in the smB isoform for point mutations in residues colocalized with Y499 (46).

We have shown that the loop 1 deletion distinguishing smA and smB isoforms introduces changes to myosin transduction that are difficult to foresee by intuition. This application demonstrates difficulties facing proactive protein engineering when apparently minor sequence changes, reasonably assumed to affect product release, in practice have wider and unanticipated effects. Protein modularity is a concept whereby function is defined by standard interchangeable modules performing specific tasks in the protein. The notion was applied years ago to myosin with the discovery of conserved proteolysis products suggesting they constitute functional domains (71,72). Functional domains defined by proteolysis proved to be of limited practical value in myosin but the idea remains inviting for use in new applications in protein engineering. Modularity mitigates the effect of a sequence change designed for one purpose spilling over into another area of protein function. This result would argue loop 1 is the interface between modules causing effects that purposefully spill over module boundaries.

CONCLUSION

Smooth muscle myosin has isoforms partitioning preferentially into tonic or phasic muscle types. Tonic muscle preferentially contains the smA isoform lacking a seven-amino-acid insert in the active site at loop 1. Phasic muscle preferentially contains the smB isoform containing the loop 1 insert. Homology modeling of smA and smB sequences with available myosin crystal structures indicates reduced loop 1 structural heterogeneity, implying reduced dynamic flexibility, in the shorter form. Nucleotide-induced fluorescence intensity increase in the highly conserved W506 occurs in all myosin isoforms previously tested implying it results from common origin within the conserved motor core. WT-smA has nucleotide-induced tryptophan fluorescence enhancement like other myosin isoforms but we showed with site-directed mutagenesis that the NST is probably not W506. Nonetheless, the additional Y499F substitution partially restores nucleotide sensitivity in W506 demonstrating Y499's predicted role as a NST facilitator. These experimental results suggest that smA and smB myosin isoforms have different influence propagating pathways

emanating from the active site. The seven-amino-acid deletion from loop 1, suggested previously to alter ATPase kinetics by interfering with ADP release, also affects distant sites in the protein by measurably altering their communication link to the active site.

SUPPLEMENTARY MATERIAL

To view all of the supplemental files associated with this article, visit www.biophysj.org.

We thank Ben Madden from the Mayo Protein Core Facility for the protein sequencing work and Sungjo Park for critically reading the manuscript.

This work was supported by National Institutes of Health, National Institute of Arthritis and Musculoskeletal and Skin Diseases grant R01AR049277 and the Mayo Foundation. Emma A. Morrison was supported in part by a summer undergraduate research fellowship from Mr. and Mrs. Norman Barker Jr.

REFERENCES

1. Lowey, S., G. S. Waller, and K. M. Trybus. 1993. Skeletal muscle myosin light chains are essential for physiological speeds of shortening. *Nature*. 365:454–456.
2. Trybus, K. M., G. S. Waller, and T. A. Chatman. 1994. Coupling of ATPase activity and motility in smooth muscle myosin is mediated by the regulatory light chain. *J. Cell Biol.* 124:963–969.
3. Babu, G. J., D. M. Warshaw, and M. Perisamy. 2000. Smooth muscle myosin heavy chain isoforms and their role in muscle physiology. *Microsc. Res. Tech.* 50:532–540.
4. Léguillette, R., F. R. Gil, and N. Zitouni. 2005. (+)Insert smooth muscle myosin heavy chain (SM-B) isoform expression in human tissues. *Am. J. Physiol.* 289:C1277–C1285.
5. Sweeney, H. L., S. S. Rosenfeld, F. Brown, L. Faust, J. Smith, J. Xing, L. A. Stein, and J. R. Sellers. 1998. Kinetic tuning of myosin via a flexible loop adjacent to the nucleotide binding pocket. *J. Biol. Chem.* 273:6262–6270.
6. Lauzon, A.-M., M. J. Tyska, A. S. Rovner, Y. Freyzon, D. M. Warshaw, and K. M. Trybus. 1998. A 7-amino-acid insert in the heavy chain nucleotide binding loop alters the kinetics of smooth muscle myosin in the laser trap. *J. Muscle Res. Cell Motil.* 19:825–837.
7. Sellers, J. R., and C. Veigel. 2006. Walking with myosin V. *Curr. Opin. Cell Biol.* 18:68–73.
8. Rovner, A. S., Y. Freyzon, and K. M. Trybus. 1997. An insert in the motor domain determines the functional properties of expressed smooth muscle myosin isoforms. *J. Muscle Res. Cell Motil.* 18: 103–110.
9. Matthew, J. D., A. S. Khromov, K. M. Trybus, A. P. Somlyo, and A. V. Somlyo. 1998. Myosin essential light chain isoforms modulate the velocity of shortening propelled by nonphosphorylated crossbridge. *J. Biol. Chem.* 273:31289–31296.
10. Arner, A., M. Lofgren, and I. Morano. 2003. Smooth, slow and smart muscle motors. *J. Muscle Res. Cell Motil.* 24:165–173.
11. Bagshaw, C. R., and D. R. Trentham. 1974. The characterization of myosin-product complexes and product-release steps during the magnesium ion-dependent adenosine triphosphate reaction. *Biochem. J.* 141:331–349.
12. Trentham, D. R., J. F. Eccleston, and C. R. Bagshaw. 1976. Kinetic analysis of ATPase mechanisms. *Q. Rev. Biophys.* 9:217–281.
13. Yount, R. G., D. Lawson, and I. Rayment. 1995. Is myosin a ''back door'' enzyme? *Biophys. J.* 68:44s–49s.
14. Geeves, M. A., R. Fedorov, and D. J. Manstein. 2005. Molecular mechanism of actomyosin-based motility. *Cell. Mol. Life Sci.* 62:1462–1477.
15. Marston, S. B., and E. W. Taylor. 1980. Comparison of the myosin and actomyosin ATPase mechanisms of the four types of vertebrate muscles. *J. Mol. Biol.* 139:573–600.
16. Taylor, R. S., and A. G. Weeds. 1976. The magnesium-ion-dependent adenosine triphosphatase of bovine cardiac myosin and its subfragment-1. *Biochem. J.* 159:301–315.
17. Fisher, A. J., C. A. Smith, J. B. Thoden, R. Smith, K. Sutoh, H. M. Holden, and I. Rayment. 1995. X-ray structures of the myosin motor domain of *Dictyostelium discoideum* complexed with MgADP.BeF_x and MgADP-AlF_4. *Biochemistry.* 34:8960–8972.
18. Werber, M. M., Y. M. Peyser, and A. Muhlrad. 1992. Characterization of stable beryllium fluoride, aluminum fluoride, and vanadate containing myosin subfragment 1-nucleotide complexes. *Biochemistry*. 31: 7190–7197.
19. Gulick, A. M., C. B. Bauer, J. B. Thoden, and I. Rayment. 1997. X-ray structures of the MgADP, MgATPγS, and MgAMPPNP complexes of the *Dictyostelium discoideum* myosin motor domain. *Biochemistry.* 36:11619–11628.
20. Peyser, Y. M., K. Ajtai, M. M. Werber, T. P. Burghardt, and A. Muhlrad. 1997. Effect of metal cations on the conformation of myosin subfragment-1-ADP-phosphate analog complexes: a near UV circular dichroism study. *Biochemistry.* 36:5170–5178.
21. Smith, C. A., and I. Rayment. 1996. X-ray structure of the magnesium(II)-ADP-vanadate complex of the dictyostelium discoideum myosin motor domain to 1.9 Å resolution. *Biochemistry*. 35:5404–5417.
22. Maruta, S., G. D. Henry, B. D. Sykes, and M. Ikebe. 1993. Formation of the stable myosin-ADP-aluminum fluoride and myosin-ADP-beryllium fluoride complexes and their analysis using ^{19}F NMR. *J. Biol. Chem.* 268:7093–7100.
23. Dominguez, R., Y. Freyzon, K. M. Trybus, and C. Cohen. 1998. Crystal structure of a vertebrate smooth muscle myosin motor domain and its complex with the essential light chain: visualization of the prepower stroke state. *Cell.* 94:559–571.
24. Goody, R. S., and W. Hofmann. 1980. Stereochemical aspects of the interaction of myosin and actomyosin with nucleotides. *J. Muscle Res. Cell Motil.* 1:101–115.
25. Peyser, Y. M., K. Ajtai, T. P. Burghardt, and A. Muhlrad. 2001. Effect of ionic strength on the conformation of myosin subfragment 1-nucleotide complexes. *Biophys. J.* 81:1101–1114.
26. Houdusse, A., V. N. Kalabokis, D. Himmel, A. G. Szent-Gyorgyi, and C. Cohen. 1999. Atomic structure of scallop myosin subfragment S1 complexed with MgADP: a novel conformation of the myosin head. *Cell.* 97:459–470.
27. Morita, F. 1967. Interaction of heavy meromyosin with substrate. *J. Biol. Chem.* 242:4501–4506.
28. Werber, M. M., A. G. Szent-Györgyi, and G. D. Fasman. 1972. Fluorescence studies on heavy meromyosin-substrate interaction. *Biochemistry.* 11:2872–2883.
29. Batra, R., and D. J. Manstein. 1999. Functional characterisation of *Dictyostelium* myosin II with conserved tryptophanyl residue 501 mutated to tyrosine. *Biol. Chem.* 380:1017–1023.
30. Werber, M. M., Y. M. Peyser, and A. Muhlrad. 1987. Modification of myosin subfragment 1 tryptophans by dimethyl(2- hydroxy-5-nitrobenzyl) sulfonium bromide. *Biochemistry.* 26:2903–2909.
31. Johnson, W. C., D. B. Bivin, K. Ue, and M. F. Morales. 1991. A search for protein structural changes accompanying the contractile interaction. *Proc. Natl. Acad. Sci. USA.* 88:9748–9750.
32. Hiratsuka, T. 1992. Spatial proximity of ATP-sensitive tryptophanyl residue(s) and Cys-697 in myosin ATPase. *J. Biol. Chem.* 267:14949–14954.
33. Papp, S., and S. Highsmith. 1993. The ATP-induced myosin subfragment-1 fluorescence intensity increase is due to one tryptophan. *Biochim. Biophys. Acta.* 1202:169–172.

34. Park, S., K. Ajtai, and T. P. Burghardt. 1996. Cleft containing reactive thiol of myosin closes during ATP hydrolysis. *Biochim. Biophys. Acta.* 1296:1–4.

35. Park, S., and T. P. Burghardt. 2000. Isolating and localizing ATP-sensitive tryptophan emission in skeletal myosin subfragment 1. *Biochemistry.* 39:11732–11741.

36. Yengo, C. M., L. R. Chrin, A. S. Rovner, and C. L. Berger. 2000. Tryptophan 512 is sensitive to conformational changes in the rigid relay loop of smooth muscle myosin during the MgATPase cycle. *J. Biol. Chem.* 275:25481–25487.

37. Bayley, P. M., E. B. Nielsen, and J. A. Schellman. 1969. The rotatory properties of molecules containing two peptide groups: theory. *J. Phys. Chem.* 73:228–243.

38. Adams, P. D., Y. Chen, K. Ma, M. G. Zagorski, F. D. Sonnichsen, M. L. McLaughlin, and M. D. Barkley. 2002. Intramolecular quenching of tryptophan fluorescence by the peptide bond in cyclic hexapeptides. *J. Am. Chem. Soc.* 124:9278–9286.

39. Gao, F., N. Bren, T. P. Burghardt, S. Hansen, R. H. Henchman, P. Taylor, J. A. McCammon, and S. M. Sine. 2005. Agonist-mediated conformational changes in acetylcholine-binding protein revealed by simulation and intrinsic tryptophan fluorescence. *J. Biol. Chem.* 280: 8443–8451.

40. Lehrer, S. S. 1971. Solute perturbation of protein fluorescence. The quenching of the tryptophyl fluorescence of model compounds and of lysozyme by iodide ion. *Biochemistry.* 10:3254–3263.

41. Yoshino, H., F. Morita, and K. Yagi. 1972. Interaction of heavy meromyosin with substrate VI. The difference absorption spectra induced by ATP analogs and chemical modification of tryptophanyl residue with 2-hydroxy-5-nitrobenzyl bromide. *J. Biol. Chem.* 72:1227–1235.

42. Bivin, D. B., S. Kubota, R. Pearlstein, and M. F. Morales. 1993. On how a myosin tryptophan may be perturbed. *Proc. Natl. Acad. Sci. USA.* 90:6791–6795.

43. Malnasi-Csizmadia, A., M. Kovacs, R. J. Woolley, S. W. Botchway, and C. R. Bagshaw. 2001. The dynamics of the relay loop tryptophan residue in the *Dictyostelium* myosin motor domain and the origin of spectroscopic signals. *J. Biol. Chem.* 276:19483–19490.

44. Park, S., and T. P. Burghardt. 2002. Tyrosine mediated tryptophan ATP sensitivity in skeletal myosin. *Biochemistry.* 41:1436–1444.

45. Burghardt, T. P., S. Park, W.-J. Dong, J. Xing, H. C. Cheung, and K. Ajtai. 2003. Energy transduction optical sensor in skeletal myosin. *Biochemistry.* 42:5877–5884.

46. Onishi, H., K. Konishi, K. Fujiwara, K. Hayakawa, M. Tanokura, H. M. Martinez, and M. F. Morales. 2000. On the tryptophan residue of smooth muscle myosin that responds to binding of nucleotide. *Proc. Natl. Acad. Sci. USA.* 97:11203–11208.

47. van Duffelen, M., L. R. Chrin, and C. L. Berger. 2004. Nucleotide dependent intrinsic fluorescence changes of W29 and W36 in smooth muscle myosin. *Biophys. J.* 87:1767–1775.

48. Weeds, A. G., and R. S. Taylor. 1975. Separation of subfragment-1 isoenzymes from rabbit skeletal muscle myosin. *Nature.* 257:54–56.

49. Pardee, J. D., and J. A. Spudich. 1982. Purification of muscle actin. *Meth. Enzymol.* 85:164–179.

50. Hu, Q., R. J. Noll, H. Li, A. Markarov, M. Hardman, and R. G. Cooks. 2005. The Orbitrap: a new mass spectrometer. *J. Mass Spectrom.* 50:430–443.

51. Eng, J. K., A. L. McCormack, and J. R. Yates. 1994. An approach to correlate tandem mass spectral data of peptides with amino acid sequences in a protein database. *J. Am. Soc. Mass Spectrom.* 5:976–989.

52. Fiske, C. H., and Y. Subbarow. 1925. The colorimetric determination of phosphorous. *J. Biol. Chem.* 66:375–400.

53. Kodama, T., K. Fukui, and K. Kometani. 1986. The initial phosphate burst in ATP hydrolysis by myosin and subfragment-1 as studied by a modified malachite green for determination of inorganic phosphate. *J. Biol. Chem.* 99:1465–1472.

54. Kouyama, T., and K. Mihashi. 1981. Fluorimetry study of *N*-(1-pyrenyl) iodoacetamide-labelled F-actin. Local structural change of actin protomer both on polymerization and on binding of heavy meromyosin. *Eur. J. Biochem.* 114:33–38.

55. Kurzawa, S. E., and M. Geeves. 1996. A novel stopped-flow method for measuring the affinity of actin for myosin head fragments using microgram quantities of protein. *J. Muscle Res. Cell Motil.* 17:669–676.

56. Conibear, P. B., and M. A. Geeves. 1998. Cooperativity between the two heads of rabbit skeletal muscle heavy meromyosin in binding to actin. *Biophys. J.* 75:926–937.

57. Criddle, A. H., M. A. Geeves, and T. Jeffries. 1985. The use of actin labelled with *N*-(1-pyrenyl)iodoacetamide to study the interaction of actin with myosin subfragments and troponin/tropomyosin. *Biochem. J.* 232:343–349.

58. Ajtai, K., S. P. Garamszegi, S. Watanabe, M. Ikebe, and T. P. Burghardt. 2004. The myosin cardiac loop participates functionally in the actomyosin interaction. *J. Biol. Chem.* 279:23415–23421.

59. Burghardt, T. P., S. Park, and K. Ajtai. 2001. Conformation of myosin interdomain interactions during contraction: deductions from proteins in solution. *Biochemistry.* 40:4834–4843.

60. Schellman, J. A. 1975. Circular dichroism and optical rotation. *Chem. Rev.* 75:323–331.

61. Badea, M. G., and L. Brand. 1979. Time-resolved fluorescence measurements. *Meth. Enzymol.* 61:378–425.

62. Ross, J. B. A., K. W. Rousslang, and L. Brand. 1981. Time-resolved fluorescence and anisotropy decay of the tryptophan in adrenocorticotropin-(1–24). *Biochemistry.* 20:4361–4369.

63. Šali, A., and T. L. Blundell. 1993. Comparative protein modelling by satisfaction of spatial restraints. *J. Mol. Biol.* 234:779–815.

64. Rayment, I., W. R. Rypniewski, K. Schmidt-Base, R. Smith, D. R. Tomchick, M. M. Benning, D. A. Winkelmann, G. Wesenberg, and H. M. Holden. 1993. Three-dimensional structure of myosin subfragment-1: a molecular motor. *Science.* 261:50–58.

65. Takashi, R., J. Duke, K. Ue, and M. F. Morales. 1976. Defining the ''fast-reacting'' thiols of myosin by reaction with 1,5 IAEDANS. *Arch. Biochem. Biophys.* 175:279–283.

66. Botts, J., R. Takashi, P. Torgerson, T. Hozumi, A. Muhlrad, D. Mornet, and M. F. Morales. 1984. On the mechanism of energy transduction in myosin subfragment 1. *Proc. Natl. Acad. Sci. USA.* 81:2060–2064.

67. Kovacs, M., F. Wang, A. Hu, Y. Zhang, and J. R. Sellers. 2003. Functional divergence of human cytoplasmic myosin II. *J. Biol. Chem.* 278:38132–38140.

68. Cremo, C., and M. Geeves. 1998. Interaction of actin with the head domain of smooth muscle myosin: implications for strain dependent ADP release in smooth muscle. *Biochemistry.* 37:1969–1978.

69. Ajtai, K., S. P. Garamszegi, S. Park, A. L. Velazquez Dones, and T. P. Burghardt. 2001. Structural characterization of β-cardiac myosin subfragment 1 in solution. *Biochemistry.* 40:12078–12093.

70. Malnasi-Csizmadia, A., R. J. Woolley, and C. R. Bagshaw. 2000. Resolution of conformational states of *Dictyostelium* myosin II motor domain using tryptophan (W501) mutants: implications for the open-closed transition identified by crystallography. *Biochemistry.* 39: 16135–16146.

71. Bálint, M., F. A. Sréter, I. Wolf, B. Nagy, and J. Gergely. 1975. The substructure of heavy meromyosin. The effect of Ca^{2+} and Mg^{2+} on the tryptic fragmentation of heavy meromyosin. *J. Biol. Chem.* 250: 6168–6177.

72. Muhlrad, A., and M. F. Morales. 1984. Isolation and partial renaturation of proteolytic fragments of the myosin head. *Proc. Natl. Acad. Sci. USA.* 81:1003–1007.